Geosciences and Engineering, Vol. 4, No. 6 (2015), pp. 81–92.

INVERSION RECONSTRUCTION OF 3D GRAVITY POTENTIAL FUNCTION INCLUDING VERTICAL DEFLECTIONS

LAJOS VÖLGYESI[1]–GYULA TÓTH[1]–MIHÁLY DOBRÓKA[2]

[1]*Department of Geodesy and Surveying, Faculty of Civil Engineering, Budapest University of Technology and Economics*
volgyesi@eik.bme.hu, gtoth@agt.bme.hu
[2]*Department of Geophysics, University of Miskolc*
dobroka@uni-miskolc.hu

Abstract. Inversion reconstruction of 3D gravity potential based on gravity data measured by gravimeters, horizontal gravity gradients and curvature data measured by torsion balance and vertical gradients, including vertical deflection data have been obtained by our 3D solution. By applying this method the potential function – apart from an additive constant – and all the first and second derivatives of this potential function (elements of the full Eötvös-tensor) can be determined not only at points of the region covered by measurements, but anywhere in the surroundings of these measurement points, using the coefficients of expansion in a series of a known set of basis function. The advantage of this method is that the solution can be performed by a significantly overdetermined inverse problem.

Computations were made for the inversion reconstruction of gravity potential at a test area where gravity, torsion balance, vertical gradient measurements and vertical deflection data were available. Gravity potential, vertical deflections and both the first and the second derivatives of the potential were determined for the whole area by this suggested method.

1. INTRODUCTION

There are more than 45,000 torsion balance measurements in a computer database in Hungary. Earlier measurements were made mainly for geophysical prospecting, but nowadays more efficient methods are applied in geophysics and instead of a geophysical application of the torsion balance measurements, geodetic applications have come to the front. Possibilities of geodetic applications of gravity gradients are continually growing [1] [2] [3] [4] [5].

Determination of the potential function has great importance because all components of the gravity vector, vertical deflection and the elements of the full Eötvös tensor can be derived from it as the first and the second derivatives of this function. Now a solution of the determination of 3D potential function is given here as an improvement on our former solution of 2D inversion [6] and [7]. Besides gravity and gravity gradients, now we have integrated vertical deflection data into the computations. Nowadays revolutionary changes are expected in geodesy because we have a new system which is capable of measuring very precise vertical deflection data with high efficiency [8].

For verification of the 3D inversion algorithm, test computations were performed at the south part of Csepel Island, a location where gravity, torsion balance, vertical gradient and vertical deflection data are available from a new model.

2. THE INVERSION ALGORITHM

Let us choose the 3D gravity potential $W(x, y, z)$ as a series expansion into a known set of basis function $\Psi_1,.\Psi_2,..., \Psi_P$:

$$W(x,y,z) = \sum_{i=1}^{N_x}\sum_{j=1}^{N_y}\sum_{k=1}^{N_z} B_n \Psi_i(x)\Psi_j(y)\Psi_k(z), \tag{1}$$

where $n = i + (j-1)N_y + (k-1)N_xN_y$ and B_n are unknown coefficients of the series expansion. In our investigations Legendre polynomials are applied as basis functions. The constant term is marked by index 1, so the possibility of $I = j = k = 1$ can be precluded, because the potential is unique apart from an additive constant.

The second derivatives of the potential Eq. (1) (the elements of the Eötvös-tensor) give the computed values of horizontal gradients W_{zx}, W_{zy}, curvature data W_{Δ}, W_{xy} and vertical gradients W_{zz} as

$$W_{zx} = \frac{\partial^2 W}{\partial x \partial z} = \sum_{i=1}^{N_x}\sum_{j=1}^{N_y}\sum_{k=1}^{N_z} B_n \Psi_i'(x)\Psi_j(y)\Psi_k'(z)\,, \tag{2}$$

$$W_{zy} = \frac{\partial^2 W}{\partial y \partial z} = \sum_{i=1}^{N_x}\sum_{j=1}^{N_y}\sum_{k=1}^{N_z} B_n \Psi_i(x)\Psi_j'(y)\Psi_k'(z)\,, \tag{3}$$

$$W_{xy} = \frac{\partial^2 W}{\partial x \partial y} = \sum_{i=1}^{N_x}\sum_{j=1}^{N_y}\sum_{k=1}^{N_z} B_n \Psi_i'(x)\Psi_j'(y)\Psi_k(z), \tag{4}$$

$$\begin{aligned} W_{\Delta} = W_{yy} - W_{xx} &= \frac{\partial^2 W}{\partial y^2} - \frac{\partial^2 W}{\partial x^2} = \\ &= \sum_{i=1}^{N_x}\sum_{j=1}^{N_y}\sum_{k=1}^{N_z} B_n \left\{ \Psi_i(x)\,\Psi_j''(y) - \Psi_i''(x)\,\Psi_j(y) \right\} \Psi_k(z)\,, \end{aligned} \tag{5}$$

$$W_{zz} = \frac{\partial^2 W}{\partial z^2} = \sum_{i=1}^{N_x}\sum_{j=1}^{N_y}\sum_{k=1}^{N_z} B_n \Psi_i(x)\,\Psi_j(y)\,\Psi_k''(z), \tag{6}$$

where the prime $'$ denotes differentiation with respect to the argument of the basis function.

The required first derivatives for the inversion algorithm are

$$W_x = \frac{\partial W}{\partial x} = \sum_{i=1}^{N_x}\sum_{j=1}^{N_y}\sum_{k=1}^{N_z} B_n \Psi_i'(x)\,\Psi_j(y)\,\Psi_k(z)\,, \tag{7}$$

$$W_y = \frac{\partial W}{\partial y} = \sum_{i=1}^{N_x}\sum_{j=1}^{N_y}\sum_{k=1}^{N_z} B_n \Psi_i(x)\,\Psi_j'(y)\,\Psi_k(z)\,, \tag{8}$$

$$W_z = \frac{\partial W}{\partial z} = \sum_{i=1}^{N_x}\sum_{j=1}^{N_y}\sum_{k=1}^{N_z} B_n \Psi_i(x)\,\Psi_j(y)\,\Psi_k'(z)\,. \tag{9}$$

Because the potential field should fulfill the Laplace-equation $\Delta W = W_{xx} + W_{yy} + W_{zz} = 0$ at each (free air) measurement point, the computed value of ΔW can be written as

$$\begin{aligned}\Delta W &= \frac{\partial^2 W}{\partial x^2} + \frac{\partial^2 W}{\partial y^2} + \frac{\partial^2 W}{\partial z^2} = \\ &= \sum_{i=1}^{N_x}\sum_{j=1}^{N_y}\sum_{k=1}^{N_z} B_n \left\{ \Psi_i''(x)\Psi_j(y)\Psi_k(z) + \Psi_i(x)\Psi_j''(y)\Psi_k(z) + \Psi_i(x)\Psi_j(y)\Psi_k''(z) \right\}.\end{aligned} \tag{10}$$

At an arbitrary measurement point $P(x_P, y_P, z_P)$ the computable data based on Eqs. (2)–(10) are:

$$^{comp.}W_{zx}^{(P)} = \sum_{n=1}^{M} B_n A_{Pn}^{(1)}\,, \tag{11}$$

$$^{comp.}W_{zy}^{(P)} = \sum_{n=1}^{M} B_n A_{Pn}^{(2)}\,, \tag{12}$$

$$^{comp.}W_{xy}^{(P)} = \sum_{n=1}^{M} B_n A_{Pn}^{(3)}\,, \tag{13}$$

$$^{comp.}W_{\Delta}^{(P)} = \sum_{n=1}^{M} B_n A_{Pn}^{(4)}\,, \tag{14}$$

$$^{comp.}W_{zz}^{(P)} = \sum_{n=1}^{M} B_n A_{Pn}^{(5)}\,, \tag{15}$$

$$^{comp.}W_{x}^{(P)} = \sum_{n=1}^{M} B_n A_{Pn}^{(6)}\,, \tag{16}$$

$$^{comp.}W_{y}^{(P)} = \sum_{n=1}^{M} B_n A_{Pn}^{(7)}\,, \tag{17}$$

$$ {}^{comp.}W_z^{(P)} = \sum_{n=1}^{M} B_n A_{Pn}^{(8)} , \tag{18} $$

$$ {}^{comp.}\Delta W^{(P)} = \sum_{n=1}^{M} B_n A_{Pn}^{(9)} , \tag{19} $$

where $M = N_x N_y N_z - 1$ is the number of coefficients of the series expansion, and

$$ A_{Pn}^{(1)} = \Psi_i'(x_P)\Psi_j(y_P)\Psi_k'(z_P) , \tag{20} $$

$$ A_{Pn}^{(2)} = \Psi_i(x_P)\Psi_j'(y_P)\Psi_k'(z_P) , \tag{21} $$

$$ A_{Pn}^{(3)} = \Psi_i'(x_P)\Psi_j'(y_P)\Psi_k(z_P) , \tag{22} $$

$$ A_{Pn}^{(4)} = \left\{ \Psi_i(x_P)\,\Psi_j''(y_P) - \Psi_i''(x_P)\,\Psi_j(y_P) \right\} \Psi_k(z_P) , \tag{23} $$

$$ A_{Pn}^{(5)} = \Psi_i(x_P)\Psi_j(y_P)\Psi_k''(z_P) , \tag{24} $$

$$ A_{Pn}^{(6)} = \Psi_i'(x_P)\Psi_j(y_P)\Psi_k(z_P) , \tag{25} $$

$$ A_{Pn}^{(7)} = \Psi_i(x_P)\Psi_j'(y_P)\Psi_k(z_P) , \tag{26} $$

$$ A_{Pn}^{(8)} = \Psi_i(x_P)\Psi_j(y_P)\Psi_k'(z_P) , \tag{27} $$

$$ A_{Pn}^{(9)} = \left\{ \Psi_i''(x_P)\Psi_j(y_P)\Psi_k(z_P) + \Psi_i(x_P)\Psi_j''(y_P)\Psi_k(z_P) + \Psi_i(x_P)\Psi_j(y_P)\Psi_k''(z_P) \right\} \tag{28} $$

are known (computable) matrix elements at the P^{th} measurement point.

The P^{th} element of the discrepancy vector of the *measured* and the *computed* data is:

$$ \varepsilon_P^{(1)} = {}^{meas.}W_{zx}^{(P)} - \sum_{n=1}^{M} B_n A_{Pn}^{(1)} , \tag{29} $$

$$ \varepsilon_P^{(2)} = {}^{meas.}W_{zy}^{(P)} - \sum_{n=1}^{M} B_n A_{Pn}^{(2)} , \tag{30} $$

$$ \varepsilon_P^{(3)} = {}^{meas.}W_{xy}^{(P)} - \sum_{n=1}^{M} B_n A_{Pn}^{(3)} , \tag{31} $$

$$ \varepsilon_P^{(4)} = {}^{meas.}W_{\Delta}^{(P)} - \sum_{n=1}^{M} B_n A_{Pn}^{(4)} , \tag{32} $$

$$ \varepsilon_P^{(5)} = {}^{meas.}W_{zz}^{(P)} - \sum_{n=1}^{M} B_n A_{Pn}^{(5)} , \tag{33} $$

$$ \varepsilon_P^{(6)} = {}^{meas.}W_{x}^{(P)} - \sum_{n=1}^{M} B_n A_{Pn}^{(6)} , \tag{34} $$

$$\varepsilon_P^{(7)} = {}^{meas.}W_y^{(P)} - \sum_{n=1}^{M} B_n A_{Pn}^{(7)}, \tag{35}$$

$$\varepsilon_P^{(8)} = {}^{meas.}W_z^{(P)} - \sum_{n=1}^{M} B_n A_{Pn}^{(8)}, \tag{36}$$

$$\varepsilon_P^{(9)} = 0 - \sum_{n=1}^{M} B_n A_{Pn}^{(9)}. \tag{37}$$

The ${}^{meas.}W_{zx}^{(P)}$, ${}^{meas.}W_{zy}^{(P)}$, ${}^{meas.}W_{xy}^{(P)}$ and the ${}^{meas.}W_{\Delta}^{(P)}$ in Eqs. (29)–(32) are torsion balance measurements, ${}^{meas.}W_{zz}^{(P)}$ in Eq. (33) are vertical gradient data, ${}^{meas.}W_z^{(P)}$ in Eq. (36) are gravity values measurable by gravimeters while ${}^{meas.}W_x^{(P)}$ in Eq. (34) and ${}^{meas.}W_y^{(P)}$ in Eq. (35) can be computed from vertical deflections. The first derivatives of the potential W from the vertical deflections are expressed as:

$$W_x = -g\xi + U_x, \tag{38}$$

$$W_y = -g\eta + U_y, \tag{39}$$

where U is normal potential [9], g is gravity and ξ, η are components of the deflection of the vertical. Equation (37) is equivalent to the Laplace-equation.

Let our inverse problem be overdetermined and let the function to be minimized be the L_2 norm of the discrepancy vector:

$$E = \sum_{s=1}^{9} \sum_{P=1}^{N_s} (\varepsilon_P^{(s)})^2, \tag{40}$$

where N_s is the number of measurements.

Let us introduce the following vector notations for measured and computed data:

$$\begin{aligned} {}^{meas.}\mathbf{d} = \{ & {}^{meas.}W_{zx}^{(1)},\ldots,{}^{meas.}W_{zx}^{(N_1)},\ldots,{}^{meas.}W_{zy}^{(1)},\ldots,{}^{meas.}W_{zy}^{(N_2)},\ldots\ldots \\ & \ldots\ldots,{}^{meas.}W_z^{(1)},\ldots,{}^{meas.}W_z^{(N_8)}, 0^{(1)},\ldots,0^{(N_9)} \} \end{aligned} \tag{41}$$

$$\begin{aligned} {}^{comp.}\mathbf{d} = \{ & {}^{comp.}W_{zx}^{(1)},\ldots,{}^{comp.}W_{zx}^{(N_1)},\ldots,{}^{comp.}W_{zy}^{(1)},\ldots,{}^{comp.}W_{zy}^{(N_2)},\ldots\ldots \\ & \ldots\ldots,{}^{comp.}W_z^{(1)},\ldots,{}^{comp.}W_z^{(N_8)},{}^{comp.}\Delta W^{(1)},\ldots,{}^{comp.}\Delta W^{(N_9)} \} \end{aligned} \tag{42}$$

All of the values of $A_{Pn}^{(i)}$ in Eqs. (20)–(28) can be written to a single coefficient matrix (to the so-called Jacobian):

$$G_{Pj}=\begin{cases} A_{Pj}^{(1)} & P \le N_1 \\ A_{Pj}^{(2)} & N_1 < P \le N_1 + N_2 \\ \vdots & \\ A_{Pj}^{(9)} & \sum_{s=1}^{8} N_s < P \le \sum_{s=1}^{9} N_s \end{cases}. \tag{43}$$

and using Eqs. (11)–(19) the vector of computed data takes the form of

$$^{comp}\mathbf{d}=\mathbf{GB}. \tag{44}$$

The discrepancy vector of measured and computed data is:

$$\boldsymbol{\varepsilon}=\ ^{meas}\mathbf{d}-\mathbf{GB}, \tag{45}$$

and substituting this into (40) one gets

$$E=(\boldsymbol{\varepsilon},\boldsymbol{\varepsilon})=\sum_{P=1}^{N} e_P^2 \tag{46}$$

for the norm, where $N=\sum_{s=1}^{9} N_s$, the total number of measurements.

The solution of this inverse problem is based on the system of conditions

$$\frac{\partial E}{\partial B_n}=0,\ (n=1,...,M) \tag{47}$$

resulting in the set of normal equations

$$\mathbf{G}^T\mathbf{GB}=\mathbf{G}^T\ ^{meas.}\mathbf{d}. \tag{48}$$

Since this inverse problem is linear, the vector **B** of series expansion coefficients can be determined by solving the above set of equations, yielding

$$\mathbf{B}=\left(\mathbf{G}^T\mathbf{G}\right)^{-1}\mathbf{G}^T\ ^{meas.}\mathbf{d}. \tag{49}$$

So the potential function in this approximation – apart from an additive constant – and all of the first and second derivatives of this potential function (the elements of the full Eötvös-tensor) can be determined not only at points of the region covered

by measurements, but anywhere in the surroundings of these measurement points using the coefficients of expansion in a series of a known set of basis function.

3. TEST COMPUTATIONS

To verify the 3D inversion algorithm, test computations were made at the south part of Csepel Island in Hungary, where gravity, torsion balance (TB) and vertical gradient (VG) measurements have been performed, furthermore vertical deflection data were available from a new model [12]. Torsion balance measurements were made here in 1950 and 30 new measurements were made in a denser net between the years 2006 and 2009, supplemented by gravity and vertical gradient observations (supported by an earlier OTKA project managed by G. Csapó [10] [11]). The location of the 4 earlier torsion balance measurement points is marked by squares, the 30 new measurement points are marked by circles and dots, while the 21 gravity measurement points are marked by crosses in Figure 1. Vertical gradient data have been measured at 27 torsion balance stations, marked by dark dots in Figure 1.

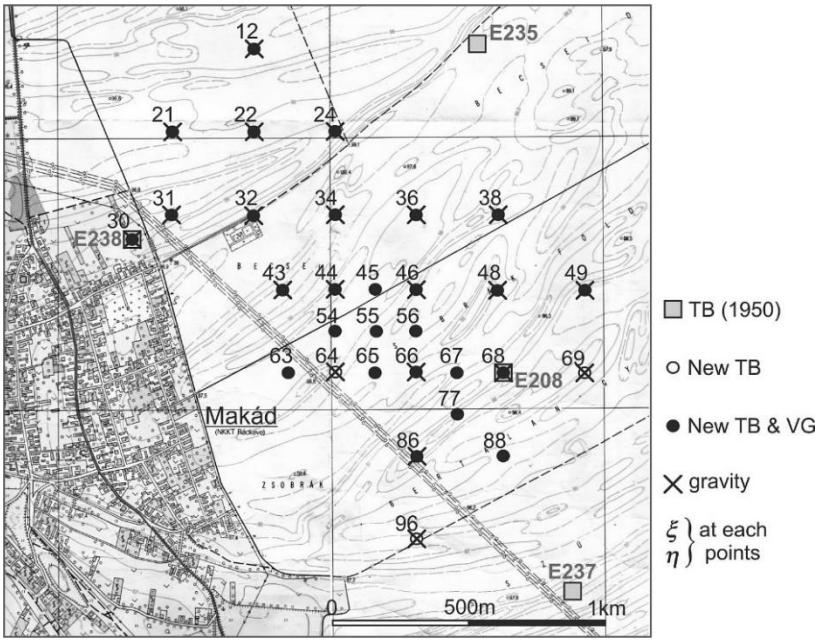

Figure 1

Torsion balance stations (marked by squares, circles, and dots), gravity measurements (marked by crosses), and vertical gradient measurements (marked by black dots) within the test area. Components ξ and η of vertical deflections are known at each point from the Hirt-model.

Deflections of the vertical have been determined for all points in the test area by the *Hirt-model* [12]. The GGMplus (Global Gravity Model plus) is constructed as a composite of data: 7 years of GRACE satellite data, 2 years of GOCE satellite, the

EGM2008 global gravity model, 7.5 arc-sec SRTM topography and 30 arc-sec SRTM30_PLUS bathymetry data, and includes North-South and East-West ξ, η components of deflections of the vertical. On the left and right side of Figure 2 ξ and η components of deflections of the vertical can be seen, respectively, in the GRS80 system in the test area (the isoline interval is 0.05 arcsec).

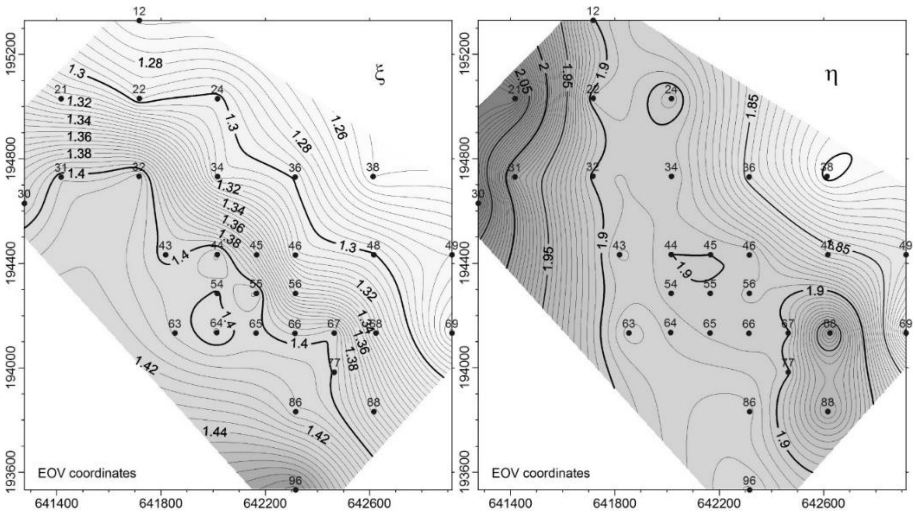

Figure 2
Vertical deflection components ξ and η within the test area from the Hirt-model. Contour interval is 0.05 arcsec

All the known horizontal gradients W_{zx} , W_{zy} , curvature data W_{xy} , W_{Δ} , vertical gradients W_{zz} and gravity values g were used as input data, but only a part of the known vertical deflection values were used as input data (as points for the training set) for the inversion; the remaining points (points of the validation set) were used for validating the computational results (15 points were considered for training, and 15 for the validation).

Our gravity and VG measurements are exremely accurate, but unfortunately torsion balance measurements have less accuracy. Vertical deflections originated from the Hirt-model [12] are available for each point, but it is important to emphasize that these are not real measurements – they do not contain the fine structure of the field, but are simply the results of a very accurate model computation. Taking this into consideration, different weights were applied for the input data: weights of the torsion balance measurements W_{zx} , W_{zy} , W_{xy} , W_{Δ} and the vertical deflection data were chosen to be 1 while the weights of gravity and VG measurements were chosen to be 10, as was the weight of the Laplace-equation.

In our solution, by substituting the computed expansion coefficients B_i from Eq. (49) into the expansion formulas (1)–(9), the potential function of the gravity field and all of its first and second derivatives were computed for the whole test area. Comparing measured and computed data, we obtained practically the same

horizontal gradients W_{zx} , W_{zy} , curvature data W_{xy} , W_{Δ} , vertical gradients W_{zz} and gravity values from the inversion as the input data of the measurements.

The relatively high spatial variations of gradients points to the need for high polinomial order in the series expansion represenation of the potential field. Our experience shows (similarly to our previous work [5]) that care should be taken in choosing the polynomial order, because when increasing its value the condition number of the normal equation increases rapidly. This can make parameter estimation (coefficients **B**) unreliable, with high estimation errors and strong correlation between some coefficients. It was earlier found that P = 18–24 can give a good compromise between resolution and stability [5], – and for this study P = 20 was applied in our computation.

From the 30 given vertical deflections 15 points were chosen as input data for the training set and are marked in Figure 3 by crosses; the remaining 15 points of the validation set as control points are marked by triangles. Our computational results are summarized in Table 1, where point number of the control points and the EOV *Y*, *X* coordinates in [m] can be found in the first three columns; then computed and given ξ , η components of the vertical deflections with their $\Delta\xi = \xi^{(comp)} - \xi^{(Hirt)}$ and $\Delta\eta = \eta^{(comp)} - \eta^{(Hirt)}$ differences can be found in the next six columns. Contour plots of $\Delta\xi$ and $\Delta\eta$ differences can be seen in Figure 3 at the same time (the contour interval is 0.05 arcsec in the figure).

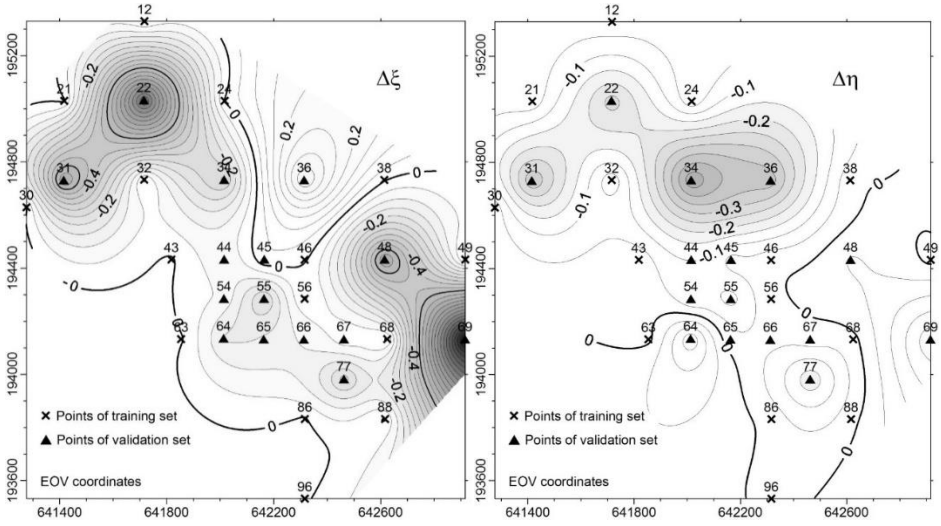

Figure3

Differences between the computed vertical deflection components by inversion and the given ξ and η determined by the Hirt-model within the test area. Points of training set are marked by crosses; points of validation set are marked by triangles.
Contour interval is 0.05 arcsec

Table1

Differences between computed and given vertical deflection data at the validation points

Point	Y [m]	X [m]	ξ (comp.) [arcsec]	ξ (Hirt) [arcsec]	Δξ [arcsec]	η (comp.) [arcsec]	η (Hirt) [arcsec]	Δη [arcsec]
31	641416.58	194729.93	0.79	1.40	–0.61	1.62	1.97	–0.35
34	642016.12	194732.41	1.00	1.31	–0.31	1.41	1.90	–0.50
36	642314.85	194730.44	1.70	1.30	0.41	1.47	1.85	–0.38
44	642015.85	194433.08	1.32	1.41	–0.09	1.80	1.90	–0.10
48	642615.88	194432.72	0.69	1.30	–0.61	1.91	1.86	0.05
64	642013.94	194135.08	1.24	1.39	–0.16	2.08	1.89	0.19
66	642313.68	194131.56	1.30	1.39	–0.09	1.87	1.90	–0.03
69	642915.90	194132.69	–0.04	1.26	**–1.30**	2.04	1.80	**0.24**
22	641716.60	195031.40	0.33	1.29	–0.96	1.62	1.89	–0.27
45	642166.00	194433.00	1.41	1.37	0.04	1.87	1.90	–0.03
54	642015.10	194284.80	1.34	1.40	–0.06	1.80	1.90	–0.10
55	642165.00	194285.00	1.15	1.41	–0.26	1.78	1.90	–0.12
65	642164.00	194132.70	1.26	1.40	–0.14	1.86	1.90	–0.04
77	642464.00	193983.00	1.12	1.40	–0.28	1.71	1.90	–0.19
67	642464.00	194133.00	1.38	1.40	–0.02	1.88	1.90	–0.02
				RMS=	**±0.36**		RMS=	**±0.16**

Root mean square (RMS) values of the differences between the vertical deflection components computed by inversion and ξ and η determined by the Hirt-model can be found in the last row of Table 1: $\mathrm{RMS}(\Delta\xi) = \pm 0.36''$ and $\mathrm{RMS}(\Delta\eta) = \pm 0.16''$. The largest error can be seen at Point 69, which is at the eastern edge of the test area, the most unfavorable place for the computation (generally extrapolation is much more unfavorable than interpolation). If we mit Point 69, the RMS values of $\Delta\xi$ and $\Delta\eta$ decrease significantly: $\mathrm{RMS}(\Delta\xi) = \pm 0.27''$, $\mathrm{RMS}(\Delta\eta) = \pm 0.15''$.

These results are quite good, compared with the accuracy of the measured vertical deflections by the QDaedalus system [8], which is about $\pm 0.1 - 0.3''$.

4. CONCLUSIONS

Inversion reconstruction of 3D gravity potential has been carried out here based on gravity data, torsion balance and vertical gradient measurements, including vertical deflection data. Computations were performed for a test area where gravity, torsion balance, vertical gradient measurements and vertical deflection data were available. Using the coefficients of a seriesexpansion of the gravity potential, both the first and the second derivatives of this potential were determined for the whole area by joint inversion.

In this study we focused on how this inversion method can be applied to the determination of vertical deflections. It can be seen that vertical deflections can be computed by this inversion method with $\pm 0.1 - 0.3''$ accuracy in our test area, which is the same as the accuracy of the vertical deflections measured by the QDaedalus system. Thus we have a very good possibility to compute vertical

deflections with suitable accuracy based on the large amount and good quality of gravity and gravity gradient data in Hungary.

5. ACKNOWLEDGEMENTS

Our investigations were supported by the National Scientific Research Fund, Project numbers OTKA K-076231 and OTKA K-109441.

6. LIST OF SYMBOLS

Symbol	Description
$A_{Pn}^{(i)}$	matrix elements at the P^{th} measurement point
B_n	coefficients of the series expansion
$\mathbf{d}$	vector of computed data
g	gravity constant
M	number of coefficients of the series expansion
N	number of measurements
$P(x_P, y_P, z_P)$	measurement point
U	normal potential
$W(x, y, z)$	gravity potential
W_{zx} , W_{zy}	horizontal gradients
W_{zz}	vertical gradients
W_{Δ} , W_{xy}	curvature data
$\boldsymbol{\varepsilon}$	discrepancy vector of measured and computed data
ξ , η	components of the deflection of the vertical
Ψ_1,Ψ_2,..., Ψ_P	set of basis function

7. REFERENCES

[1] VÖLGYESI, L.: Local geoid determinations based on gravity gradients. *Acta Geodaetica et Geophysica Hungarica*, 2001, 36, 153–162.

[2] VÖLGYESI, L.: Deflections of the vertical and geoid heights from gravity gradients. *Acta Geodaetica et Geophysica Hungarica*, 2005, 40, 147–159.

[3] VÖLGYESI, L.–TÓTH, GY.–CSAPÓ, G.–SZABÓ, Z.: The present state of geodetic applications of Torsion balance measurements in Hungary. *Geodézia és Kartográfia*, 2005, 57 (5), 3–12 (in Hungarian with English abstract).

[4] VÖLGYESI, L.–TÓTH, GY.–CSAPÓ, G.: Determination of gravity field from horizontal gradients of gravity. *Acta Geodaetica et Geophysica Hungarica*, 2007, 42 (1), 107–117.

[5] VÖLGYESI, L.–DOBRÓKA, M.–ULTMANN, Z.: Determination of vertical gradients of gravity by series expansion based inversion. *Acta Geodaetica et Geophysica Hungarica*, 2012, 47 (2),233–244.

[6] DOBRÓKA, M.–VÖLGYESI, L.: Inversion reconstruction of gravity potential based on torsion balance measurements. *Geomatikai Közlemények*, VIII, 2008, 223–230 (in Hungarian with English abstract).
[7] DOBRÓKA, M.–VÖLGYESI, L.: Inversion reconstruction of gravity potential based on gravity gradients. *Mathematical Geosciences*, 2008, 40 (3), 299–311.
[8] BÜRKI, B.–GUILLAUME,S.–SORBER, P.–PETER, O. H.: DAEDALUS: A Versatile Usable Digital Clip-on Measuring System for Total Stations. *2010 International Conference on Indoor Positioning and Indoor Navigation (IPIN)*, 15–17 September 2010, Zürich, Switzerland.
[9] TORGE, W.: *Gravimetry*. Walter de Gruyter, Berlin–New York, 1989.
[10] CSAPÓ, G.–ÉGETŐ, CS.–KLOSKA, K.–LAKY, S.–TÓTH, GY.–VÖLGYESI, L.:Test measurements by torsion balance and gravimeters in view of geodetic application of torsion balance data. *Geomatikai Közlemények*, 2009, XII, 91–100 (in Hungarian with English abstract).
[11] CSAPÓ, G.–LAKY, S.–ÉGETŐ, CS.–ULTMANN, Z.–TÓTH, GY.–VÖLGYESI, L.: Test measurements by Eötvös-torsion balance and gravimeters. *Periodica Polytechnica Civil Engineering*, 2009, 53 (2), 75–80.
[12] HIRT, C. S.–CLAESSENS, J.–FECHER, T.–KUHN, M.–PAIL, R.–REXER, M.: New ultra-high resolution picture of Earth's gravity field. *Geophysical Research Letters*, 2013, 40 (16), 4279–4283.